

Dynamic model of an omnidirectional vehicle for an unified task-space control in mobile manipulators

J. Obregon-Flores A. Morales-Díaz

*Centro de Investigación y de Estudios Avanzados del Instituto
Politécnico Nacional Unidad Saltillo
Ramos Arizpe, Coah. 25900, México
Phone number: +52-844-4389600 Ext. 8500
e-mail: {jonathan.obregon, america.morales}@cinvestav.mx.*

Abstract.

A common strategy to control an omnidirectional mobile manipulator is considering the mobile part as an extension of the generalized coordinates of the robot. Therefore, it must be assumed that the robot's vehicle can move in those coordinates, regardless of the configuration of its wheels. To achieve that, a relationship between the wheels motion and vehicle's motion must be established. Fortunately, most closed-architecture mobile robots already establish this relationship, unlike experimental open-architecture mobile robots. This relationship has been issued by several contributions, for their specific case of study, with each of them showing a particular mapping operator that relates the velocities and forces between the wheels and the vehicle. However, it is rather counterintuitive to know how the mapping operators were obtained for a particular case, whose shape depends on the vehicle's parameters and wheels configuration. In this work, we introduce a methodology to obtain a force-mapping operator for an omnidirectional vehicle, which was useful to simulate a task-space control at torque level for a mobile operator, and to implement a torque-level tracking control for a Kuka-Youbot's omnidirectional base.

Keywords: Omnidirectional Mobile Manipulator, Dynamic Model, Task Space Control.

1. INTRODUCTION

The operational area of mobile manipulators is not restricted by a fixed inertial base, so their redundancy is generally greater than inertial robots. This can be exploited in order to accomplish a set of simultaneous tasks; such as maintaining the manipulator's end-effector lifting an object in a desired position and orientation while the vehicle moves through a given trajectory. Controlling a mobile manipulator as a whole system requires that the motion coordinates of the vehicle are the same as those of the manipulator arm, thus requiring the vehicle's wheels to move in a synchronized manner to achieve such a desired motion. This can be achieved by finding a relationship between velocities or forces in the wheels and in the vehicle, which depends on the kind of wheels and their position on the vehicle. Such relationship can be described by a mapping operator for velocities and forces. Therefore, the whole robot can be modeled and controlled. Some related works have emerged proposing unified kinematics models for mobile manipulators, such as Sharma et al. (2012), which deploys an inverse kinematics solver that generates all possible solutions to determine the required base and joint positions for a desired end-effector pose. In Mirelez et al. (2016) the unified kinematic

model of a mobile manipulator is derived considering the DOF of the omnidirectional vehicle as a part of the kinematic chain, and using a quaternion parametrization to represent the end-effector's attitude. Also, the unified dynamics of the mobile manipulator is worth being considered for path planning, motion optimization, feedback control algorithm design, and hierarchies for dynamically feasible tasks (Estopier et al. (2014)). Related works such as Changwu Qiu et al. (2008), propose a methodology to obtain the dynamic model of an omnidirectional dual arm mobile manipulator using spatial notation derived from the Lie group theory. However, the control of the unified system is not discussed. In Watanabe et al. (2000), while the model and control of a three-wheeled omnidirectional mobile manipulator is derived, the dynamic model of the vehicle is not deeply discussed, nor the methodology to obtain the operator they used to map between the wheels torques to the force quantities that belong to the same space where the vehicle moves. Some of the aforementioned authors have contributed to the kinematic and dynamic modeling of mobile manipulators for multiple applications. Even though, the methodology to obtain the force mapping operator is not discussed, which is always different depending on the wheel's configuration of the robot.

In this work we propose a methodology to obtain a force mapping operator from the dynamic model of a four-wheeled omnidirectional vehicle, which can be assumed as a rigid body subjected to exogenous wrenches with a holonomic constraint represented by a horizontal flat floor. We adopted spatial notation and operators obtained from Lie algebra, simplifying the notation of equations of motion and mapping operators.

This operator was necessary for a torque-level control of the omnidirectional vehicle, such that it was possible to control the mobile manipulator a whole system.

This paper is organized as follows. Section 2 formulates the dynamic model of the omnidirectional vehicle, from which the force-mapping operator was derived. In Section 3 we use the force mapping operator to include the wheels torques in the general equation of motion of the mobile manipulator. In 4 the task-space control framework is briefly recalled, and simulated in Section 5. Experimental results are shown in Section 6, and concluding remarks in Section 7.

2. DYNAMIC MODEL OF THE OMNIDIRECTIONAL VEHICLE

Let assign frames to the wheels Σ_{wi} and to the vehicle's center of mass Σ_b as in Figure (1)

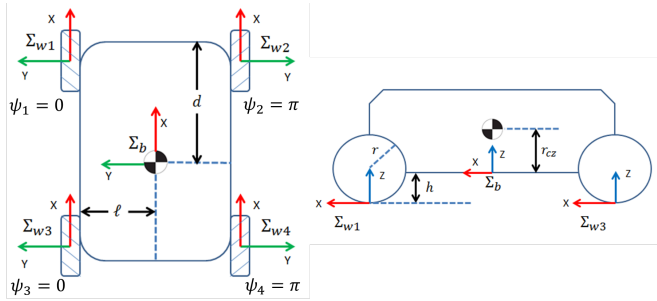


Figure 1. Vehicle's frames.

Therefore, by following Figure (1), we define $\mathbf{d}_b^{wi} = [d \ \ell \ h]^T$ as the distance between Σ_{wi} and Σ_b , and their orientation change is given by the rotation matrices \mathbf{R}_b^{wi} for $i = 1 \dots w$, where w denotes the number of wheels.

The resulting wrench, in reference to the vehicle's frame, $\mathbf{F} \in \mathbb{R}^6$ is the addition of each wrench produced by the wheels $\mathbf{F}_{wi} \in \mathbb{R}^6$ for $i = 1 \dots w$. Therefore, in order to represent \mathbf{F}_{wi} with respect to Σ_b , coordinates transformation operators are needed, which are defined in Park et al. (1995) as the linear mapping between the Lie group elements $\mathbf{X} \in SE(3)$, and the elements of its Lie algebra $\nu \in se(3)$, by the adjoint representation $\mathbf{Ad}_X(\nu)$, where \mathbf{X} is composed by the ordered pair (\mathbf{R}, \mathbf{d}) , with $\mathbf{R} \in SO(3)$ and $\mathbf{d} \in \mathbb{R}^3$, where the algebra of the elements of $SO(3)$, denoted by $so(3)$, is defined by a skew symmetric matrix $\mathbf{S}(\omega)$, which can also be regarded as a vector $\omega \in \mathbb{R}^3$. On the other hand, the elements in $se(3)$ are denoted by the ordered pair $(\mathbf{S}(\omega), \mathbf{v})$, which can also

be regarded as a vector $\nu = [\omega \ \mathbf{v}]^T \in \mathbb{R}^6$ describing the twist of a body. Therefore the adjoint map of the $SE(3)$ element $\mathbf{X} = (\mathbf{R}, \mathbf{d})$, acting on its $se(3)$ element $\nu = (\omega, \mathbf{v})$ is given by $\mathbf{Ad}_X(\nu) = \mathbf{X}\nu\mathbf{X}^{-1}$, i.e.,

$$\mathbf{Ad}_X(\nu) = (\mathbf{R}\omega, \mathbf{d} \times \mathbf{R}(\omega + \mathbf{v})), \quad (1)$$

which can be expressed as a 6×6 matrix

$$\mathbf{Ad}_X(\nu) = \begin{bmatrix} \mathbf{R} & \mathbf{0} \\ \mathbf{S}(\mathbf{d})\mathbf{R}^T & \mathbf{R} \end{bmatrix} \begin{bmatrix} \omega \\ \mathbf{v} \end{bmatrix}, \quad (2)$$

which can also be written as follows

$$\mathbf{Ad}_X(\nu)^{-1} = \begin{bmatrix} \mathbf{R}^T & -\mathbf{R}^T\mathbf{S}(\mathbf{d}) \\ \mathbf{0} & \mathbf{R}^T \end{bmatrix} \begin{bmatrix} \mathbf{v} \\ \omega \end{bmatrix}. \quad (3)$$

A dual operator \mathbf{Ad}_X^* acting on the elements of the cotangent space of $SE(3)$, denoted by $se^*(3)$, has a matrix representation given by the transpose of \mathbf{Ad}_X^{-1} , for the elements $\mathbf{f} = (\mathbf{f}, \mathbf{n}) \in se^*(3)$, representing force and moment vectors, which constitutes the wrench of a body. This operator is defined as

$$\mathbf{Ad}_X^*(\mathbf{f}) = \begin{bmatrix} \mathbf{R}^T & \mathbf{0} \\ -\mathbf{R}^T\mathbf{S}(\mathbf{d}) & \mathbf{R}^T \end{bmatrix} \begin{bmatrix} \mathbf{f} \\ \mathbf{n} \end{bmatrix}. \quad (4)$$

Defining $\mathbf{Ad}_X^{-1} \triangleq \mathbf{G} \in \mathbb{R}^{(6 \times 6)}$ and $\mathbf{Ad}_X^* \triangleq \mathbf{G}^T \in \mathbb{R}^{(6 \times 6)}$, the total input wrench of the vehicle is now given as:

$$\mathbf{F} = \sum_{i=1}^w \mathbf{G}_i^T \mathbf{F}_{wi}. \quad (5)$$

The wrench in each wheel is denoted by $\mathbf{F}_{wi} = [f_{xi}, f_{yi}, f_{zi}, \tau_{xi}, \tau_{yi}, \tau_{zi}]^T$, and is defined according to Figure (2), where, for each wheel to move along x , the

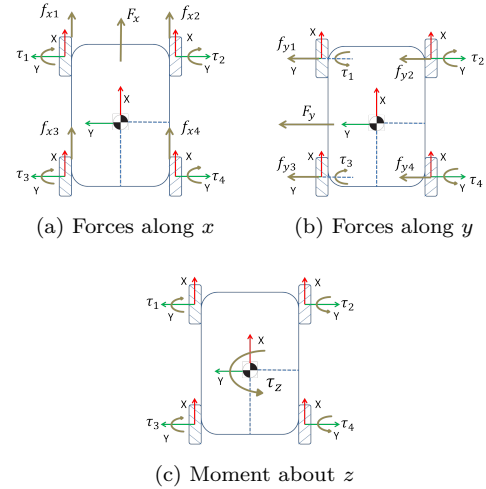


Figure 2. Vehicle's forces distribution

force is $f_{xi} = \frac{1}{r}\tau_{mi}$. Meanwhile, motion along y , implies $f_{yi} = \frac{-\tau_{m1} - \tau_{m2} + \tau_{m3} + \tau_{m4}}{4r}$, for $i = 1, 3$ and $f_{yi} = \frac{\tau_{m1} + \tau_{m2} - \tau_{m3} - \tau_{m4}}{4r}$ for $i = 2, 4$. The rollers of the mecanum wheels permits lateral displacement but its effects are neglected in this work, because the relationship between torques and wheels radius, and their individual rotation combination, is what mostly describes the resulting wrench of each wheel. The contact forces of each wheel

f_{zi} are normal to the floor plane and keeps the base at floor level. The wheels are fixed on the base such that their orientation does not change, then $\tau_{xi} = \tau_{zi} = 0$. The torque occurring at τ_{yi} that yields f_{xi} is what rotates the wheels, but their frame is fixed and does not rotate because of the vehicle constraint, therefore $\tau_{yi} = 0$. So, \mathbf{F}_{wi} is denoted as follows:

$$\mathbf{F}_{wi} = \left[\frac{1}{r}\tau_{mi}, \frac{-\tau_{m1}-\tau_{m2}+\tau_{m3}+\tau_{m4}}{4r}, f_{zi}, 0, 0, 0 \right]^T, \quad (6)$$

for $i = 1, 3$,

$$\mathbf{F}_{wi} = \left[\frac{1}{r}\tau_{mi}, \frac{\tau_{m1}+\tau_{m2}-\tau_{m3}-\tau_{m4}}{4r}, f_{zi}, 0, 0, 0 \right]^T, \quad (7)$$

for $i = 2, 4$.

We can group the exogenous motor torques in vectors according to how they produce motion in a certain generalized coordinate direction

$$\boldsymbol{\tau}_a = \begin{bmatrix} \tau_{m1} \\ \tau_{m2} \\ \tau_{m3} \\ \tau_{m4} \end{bmatrix}, \quad \boldsymbol{\tau}_b = \frac{1}{4} \begin{bmatrix} -\tau_{m1} - \tau_{m2} + \tau_{m3} + \tau_{m4} \\ \tau_{m1} + \tau_{m2} - \tau_{m3} - \tau_{m4} \\ -\tau_{m1} - \tau_{m2} + \tau_{m3} + \tau_{m4} \\ \tau_{m1} + \tau_{m2} - \tau_{m3} - \tau_{m4} \end{bmatrix}, \quad (8)$$

$$\boldsymbol{\tau}_c = [f_{z1} \ f_{z2} \ f_{z3} \ f_{z4}]^T.$$

with $\boldsymbol{\tau}_a$ and $\boldsymbol{\tau}_b$ containing torques that produce motion along the x -axis and y -axis respectively, $\boldsymbol{\tau}_c$ contains the forces spanning at the contact point of the wheels.

From (6), (7) and considering (8), we can relate how torques produce motion in a certain generalized coordinate direction

$$\mathbf{f}_{x|\tau_i} = \left[\frac{1}{r} \ 0 \ 0 \ 0 \ 0 \ 0 \right]^T \tau_{ai} = \boldsymbol{\Lambda}_x \tau_{ai}, \quad (9)$$

$$\mathbf{f}_{y|\tau_i} = \left[0 \ \frac{1}{r} \ 0 \ 0 \ 0 \ 0 \right]^T \tau_{bi} = \boldsymbol{\Lambda}_y \tau_{bi}, \quad (10)$$

$$\mathbf{f}_{z|\tau_i} = \left[0 \ 0 \ 1 \ 0 \ 0 \ 0 \right]^T \tau_{ci} = \boldsymbol{\Lambda}_z \tau_{ci}, \quad (11)$$

for $i = 1 \dots w$.

Considering equation (5), torque-to-wrench mapping operators for each of the torque input vectors $\boldsymbol{\tau}_a$, $\boldsymbol{\tau}_b$, $\boldsymbol{\tau}_c$, can be derived as follows:

$$\mathbf{a}_i \tau_{ai} = \mathbf{G}_i^T \boldsymbol{\Lambda}_x \tau_{ai},$$

$$\mathbf{b}_i \tau_{bi} = \mathbf{G}_i^T \boldsymbol{\Lambda}_y \tau_{bi}, \quad (12)$$

$$\mathbf{c}_i \tau_{ci} = \mathbf{G}_i^T \boldsymbol{\Lambda}_z \tau_{ci},$$

for $i = 1 \dots w$.

At this point, we define the operators \mathbf{A} , \mathbf{B} , $\mathbf{C} \in \mathbb{R}^{(6 \times w)}$, such that we rewrite (12) as follows:

$$\mathbf{A} \boldsymbol{\tau}_a = [\mathbf{a}_1 \ \mathbf{a}_2 \ \mathbf{a}_3 \ \mathbf{a}_4] \boldsymbol{\tau}_a, \quad (13)$$

$$\mathbf{B} \boldsymbol{\tau}_b = [\mathbf{b}_1 \ \mathbf{b}_2 \ \mathbf{b}_3 \ \mathbf{b}_4] \boldsymbol{\tau}_b, \quad (14)$$

$$\mathbf{C} \boldsymbol{\tau}_c = [\mathbf{c}_1 \ \mathbf{c}_2 \ \mathbf{c}_3 \ \mathbf{c}_4] \boldsymbol{\tau}_c, \quad (15)$$

Therefore the total wrench of the vehicle can also be described as:

$$\mathbf{F} = \mathbf{A} \boldsymbol{\tau}_a + \mathbf{B} \boldsymbol{\tau}_b + \mathbf{C} \boldsymbol{\tau}_c, \quad (16)$$

where \mathbf{A} and \mathbf{B} , map the exogenous torques from the motors to a wrench of generalized forces of the mobile base. After a few operations and simplifications, equation (16) can be written as:

$$\mathbf{F} = \mathbf{J} \boldsymbol{\tau}_m + \mathbf{C} \boldsymbol{\tau}_c, \quad (17)$$

$$\mathbf{F} = \mathbf{F}_m + \mathbf{F}_c, \quad (18)$$

with $\boldsymbol{\tau}_m = \boldsymbol{\tau}_a$, and $\mathbf{J} \in \mathbb{R}^{(6 \times w)}$ is a matrix of torques distribution that computes the input wrench \mathbf{F}_m that directly spans from exogenous torque inputs. On the other hand \mathbf{C} is the operator that maps the exogenous restrictive forces $\boldsymbol{\tau}_c$ to a restrictive wrench \mathbf{F}_c constraining the motion of the vehicle. The rank of \mathbf{C} represents the dimension of constrained motions of the vehicle. Then, the rank of a null-space projector of \mathbf{C} , denoted by \mathbf{N}_c represents the dimension of admissible motion of a body. Hence $\rho(\mathbf{N}_c) = m - r$, with $m = 6$ and $r \leq 6$, where if $r = 0$ the body is free to move in the space, and if $r = 6$ the body is fully constrained and cannot move. The restriction condition, in terms of Power transmission, establishes that for all restricted coordinate i , $F_i \nu_i = 0$, hence $\nu_i = \dot{\nu}_i = 0$. We can write a motion restriction expression by using the operator \mathbf{C} to map the constraint velocities and accelerations,

$$\mathbf{v}_c = \mathbf{C}^T \boldsymbol{\nu} = 0, \quad (19)$$

$$\dot{\mathbf{v}}_c = \mathbf{C}^T \dot{\boldsymbol{\nu}} + \dot{\mathbf{C}}^T \boldsymbol{\nu} = 0. \quad (20)$$

The restriction is time involutive due to the fact that it is holonomic, therefore $\dot{\mathbf{C}} = 0$. The vector $\boldsymbol{\nu}$ is the twist of the vehicle, and \mathbf{v}_c , $\dot{\mathbf{v}}_c \in \mathbb{R}^w$ are respectively the velocities and accelerations of the wheels constrained by the floor. On the other hand, we can find that

$$\boldsymbol{\nu}_c = \mathbf{C} \mathbf{v}_c = [0 \ 0 \ \nu_z \ \omega_x \ \omega_y \ 0]^T, \quad (21)$$

with $\boldsymbol{\nu}_c$ standing for the constraint twist.

We can describe the dynamics of a rigid body with its equation of motion

$$\mathbf{M} \dot{\boldsymbol{\nu}} + \mathbf{h}(\boldsymbol{\theta}, \boldsymbol{\nu}) = \mathbf{F}, \quad (22)$$

with \mathbf{M} representing the spatial inertia matrix of a rigid body, and $\mathbf{h}(\boldsymbol{\theta}, \boldsymbol{\nu}) = \mathbf{C}_c(\boldsymbol{\theta}, \boldsymbol{\nu}) \boldsymbol{\nu} + \mathbf{g}(\boldsymbol{\theta})$ containing the centrifugal forces, the effects of Coriolis, and gravity wrench. By substituting (17) in (22), we express the model of a rigid body as that of the vehicle.

$$\mathbf{M} \dot{\boldsymbol{\nu}} + \mathbf{h}(\boldsymbol{\theta}, \boldsymbol{\nu}) = \mathbf{J} \boldsymbol{\tau}_m + \mathbf{C} \boldsymbol{\tau}_c. \quad (23)$$

To describe the dynamic model of the vehicle together with its restriction, we need to consider the acceleration constraint described by the second order kinematic constraint from equation (20). Both equations can be described in matrix form as follows:

$$\begin{bmatrix} \mathbf{M} \dot{\boldsymbol{\nu}} - \mathbf{C} \boldsymbol{\tau}_c \\ -\mathbf{C}^T \dot{\boldsymbol{\nu}} \end{bmatrix} = \begin{bmatrix} \mathbf{J} \boldsymbol{\tau}_m - \mathbf{h}(\boldsymbol{\theta}, \boldsymbol{\nu}) \\ \dot{\mathbf{C}}^T \boldsymbol{\nu} \end{bmatrix}$$

$$\begin{bmatrix} \mathbf{M} & -\mathbf{C} \\ -\mathbf{C}^T & \mathbf{0} \end{bmatrix} \begin{bmatrix} \dot{\boldsymbol{\nu}} \\ \boldsymbol{\tau}_c \end{bmatrix} = \begin{bmatrix} \mathbf{J} \boldsymbol{\tau}_m - \mathbf{h}(\boldsymbol{\theta}, \boldsymbol{\nu}) \\ \dot{\mathbf{C}}^T \boldsymbol{\nu} \end{bmatrix}, \quad (24)$$

where, in order to solve for $[\dot{\boldsymbol{\nu}} \ \boldsymbol{\tau}_c]^T$ we must invert the left part of equation (24), which is a square block matrix and can be inverted using Schur complements and some properties of square block matrices. Leading to:

$$\begin{bmatrix} \mathbf{M} & -\mathbf{C} \\ -\mathbf{C}^T & \mathbf{0} \end{bmatrix}^{-1} = \quad (25)$$

$$\begin{bmatrix} \mathbf{M}^{-1} - \mathbf{M}^{-1} \mathbf{C} [\mathbf{C}^T \mathbf{M}^{-1} \mathbf{C}]^{-1} \mathbf{C}^T \mathbf{M}^{-1} & -\mathbf{M}^{-1} \mathbf{C} [\mathbf{C}^T \mathbf{M}^{-1} \mathbf{C}]^{-1} \\ -[\mathbf{C}^T \mathbf{M}^{-1} \mathbf{C}]^{-1} \mathbf{C}^T \mathbf{M}^{-1} & -[\mathbf{C}^T \mathbf{M}^{-1} \mathbf{C}]^{-1} \end{bmatrix},$$

where $M_c^{-1} = [C^T M^{-1} C]^{-1}$ and the off diagonal elements of the matrix are the M -weighted left pseudo-inverse of C and its transpose:

$$C_M^+ = M_c^{-1} C^T M^{-1} \in \mathbb{R}^{(w \times 6)}, \quad (26)$$

$$C^\# = [C_M^+]^T = M^{-1} C M_c^{-1} \in \mathbb{R}^{(6 \times w)}, \quad (27)$$

where $C_M^+ C = I$ and $C^T C^\# = I$. Therefore a null-space projector of C projecting the residual constrained motion dynamics into admissible motion, takes its form as:

$$N_c = I - C C_M^+ \in \mathbb{R}^{(6 \times 6)}, \quad (28)$$

fulfilling both $N_c C = 0$ and $C_M^+ N_c = 0$. Then the matrix of (25) can be simplified as:

$$\begin{bmatrix} M & -C \\ -C^T & \mathbf{0} \end{bmatrix}^{-1} = \begin{bmatrix} N_c^T M^{-1} & -C^\# \\ -C_M^+ & -M_c^{-1} \end{bmatrix}. \quad (29)$$

Now, the solution for $[\dot{\nu} \ \tau_c]^T$ from equation (24) can be written as:

$$\dot{\nu} = N_c^T M^{-1} (J \tau_m - h(\theta, \nu)), \quad (30)$$

$$\tau_c = -C_M^+ (J \tau_m - h(\theta, \nu)), \quad (31)$$

From (30) we can solve for τ_m which is the active force input vector of this system:

$$M \dot{\nu} = N_c^T (J \tau_m - h(\theta, \nu)),$$

$$N_c^T J \tau_m = M \dot{\nu} + N_c^T h(\theta, \nu),$$

where it follows that:

$$J_b \triangleq N_c^T J \in \mathbb{R}^{(6 \times w)}, \quad (32)$$

is the operator that distributes the wheels torques to a constrained wrench of generalized coordinates for the floor-constrained vehicle: $F = J_b \tau_m$. Continuing solving for τ_m

$$J_b \tau_m = M \dot{\nu} + N_c^T h(\theta, \nu), \quad (33)$$

$$\tau_m = J_b^+ (M \dot{\nu} + N_c^T h(\theta, \nu)), \quad (34)$$

we conversely find that J_b^+ maps the exogenous generalized wrench to wheels torques. If solving equation (33) for $\dot{\nu}$ it is possible to know the generalized output of the system:

$$\dot{\nu} = M^{-1} (J_b \tau_m - N_c^T h(\theta, \nu)), \quad (35)$$

3. DYNAMIC MODEL OF THE MOBILE MANIPULATOR

The direct kinematics of the mobile manipulator are obtained as in Mirelez et al. (2016) also with quaternion parametrization for the end-effector pose. The direct dynamics of the mobile manipulator arm of 8 DOF are derived using spatial notation and a recursive Newton-Euler algorithm (Featherstone et al. (2000)), leading to:

$$H(q) \ddot{q} + h(q, \dot{q}) + D \dot{q} = \tau, \quad (36)$$

where $\tau = [f_b \ \tau_q]^T \in \mathbb{R}^n$ are the generalized forces of the mobile manipulator, which are computed as:

$$\begin{bmatrix} f_b \\ \tau_q \end{bmatrix} = \begin{bmatrix} J_b & \mathbf{0} \\ \mathbf{0} & I \end{bmatrix} \begin{bmatrix} \tau_m \\ \tau_q \end{bmatrix} \quad (37)$$

where $n = \dim(cs)$, $f_b \in \mathbb{R}^{(m-r)}$ and $\tau_q \in \mathbb{R}^{(n-(m-r))}$, denoting the generalized forces of the vehicle and manipulator respectively. $J_b \in \mathbb{R}^{((m-r) \times w)}$ is full rank, The generalized positions, velocities and accelerations are respectively described by q , \dot{q} and \ddot{q} . Where $q \in cs$ with $cs = SE(2) \times \mathbb{T}^{(n-(m-r))}$. $H \in \mathbb{R}^{(n \times n)}$ is the inertia matrix, which is symmetric and positive definite, $h \in \mathbb{R}^n$ is the vector of Coriolis, centrifugal forces and gravity, $D \in \mathbb{R}^{(n \times n)}$ is a diagonal matrix of viscous friction coefficients.

4. TASK SPACE CONTROL IN TORQUE MODE

In order to control the position and velocity of the end-effector spatial coordinates, we must define its pose x as a function of the generalized coordinates of the robot

$$x = f(q), \quad (38)$$

where $x = [p \ \theta]$, with $p = [x \ y \ z] \in \mathbb{R}^3$ representing the end effector position, and $\theta = [Q_0 \ Q_1 \ Q_2 \ Q_3] \in \mathbb{S}^3$ the end-effector attitude with quaternion parametrization. The pose time derivative is defined as:

$$\dot{x} = J_a(q) \dot{q}, \quad (39)$$

where $J_a(q)$ is the analytical Jacobian matrix.

A task is defined as:

$$e = x - x_d, \quad (40)$$

which if twice differentiated, it takes the following form

$$\ddot{e} = J \ddot{q} + \dot{J} \dot{q} - \ddot{x}_d. \quad (41)$$

We can relate equation (41) with the dynamics of the mobile manipulator by solving for \ddot{q} in equation (36), yielding:

$$\ddot{e} = JH^{-1}(\tau - h) + \dot{J} \dot{q}. \quad (42)$$

Defining $Q = JH^{-1}$, $\mu = Qh - \dot{J} \dot{q}$ and solving (42) for τ , yields:

$$\tau = Q^{\#H}(\ddot{e} + \mu), \quad (43)$$

where $Q^{\#H}$ is a left pseudo-inverse of Q weighted by H , τ is the control input that contains the generalized forces/torques of the robot, such as the vehicle's wrench that is mapped by J_b^+ to the required wheels torques, \ddot{e} is the second order reference nominal control in the task space and defined as:

$$\ddot{e} = -K_p e - K_v \dot{e} + \ddot{x}_d, \quad (44)$$

where K_p and K_v are diagonal constant gain matrices defining an exponential convergence of the error.

5. SIMULATIONS

Simulations of a computed torque controller for the dynamic model of an omnidirectional mobile manipulator of 8 degrees-of-freedom, shows the torque requirements of all robot actuators including the wheels, they are computed from the control input of generalized forces through the mapping operator J_b^+ , yielding torque inputs necessary to accomplish the given task. At $t = 0$, the end-effector pose is $x_0 = [0.143 \ 0 \ 0.648 \ 1 \ 0 \ 0 \ 0]$. The first stage of the task for the end-effector is a set-point regulation, beginning at $t \geq 0$ and specified by $x_{r_d} = [p_{r_d} \ \theta_{r_d}]$, where $p_{r_d} = [5 \ 3 \ 0.4]$ meters and $\theta_{r_d} =$

$[0.7065 \ 0 \ 0.7065 \ 0]$. After $t > 15$, the second stage becomes a position tracking task for the end-effector: $\mathbf{p}_{t_d} = [4 + 2 \sin(t/2) \ 4 + \sin(t) \ 0.4]$, $\dot{\mathbf{p}}_{t_d} = [\cos(t/2) \ \cos(t) \ 0]$, $\ddot{\mathbf{p}}_{t_d} = \left[\frac{-\sin(t/2)}{2} \ -\sin(t) \ 0 \right]$, keeping a new fixed orientation: $\boldsymbol{\theta}_{t_d} = [1 \ 0 \ 0 \ 0]$. The deployed control law is given in (43).

Figure (3a) shows the overall path generated by the desired trajectory and the path followed by the robot in the xy plane. The first stage ends when $t > 15$, at this time, the end-effector have already reached \mathbf{x}_r . The second stage begins with a sudden motion towards the lemniscata path \mathbf{x}_t and starts following it. Figure (3b) shows that the error asymptotically converges to zero in the first stage, unlike in the second stage where the error does not tend to zero, following the lemniscata with a constant offset. This can be explained by virtue of the end-effector desired pose whose coordinates to be tracked are only x_d and y_d , while simultaneously keeping at z_d and $\boldsymbol{\theta}_d$. This may cause conflict when trying to reach all coordinates simultaneously, which it is not feasible in all cases. Figure (4) shows the generalized forces for the robot's vehicle given by the controller. It can be seen large peaks of force magnitudes at $t > \epsilon$ when the error is maximal, and at $t > 15$ the second stage begins, inducing another peak of forces, indicating that the robot begins to move again from a steady state. Figure (5) shows the required torque inputs for the robot's vehicle that are equivalent to its generalized control input.

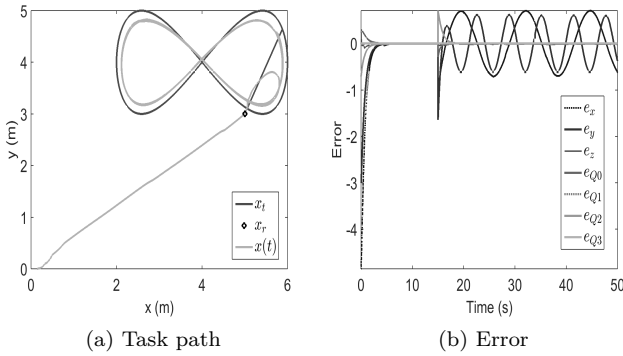


Figure 3. Task execution path.

6. EXPERIMENTS

Experiments were conducted on a Kuka Youbot with a Mini-ITX board as on-board computer in the omnidirectional vehicle, Figure (6). Processor: Intel Atom™ Dual Core D510 (1M Cache, 2 x 1.66 GHz). RAM Memory: 2GB single-channel DDR2 667MHz. Graphics: Embedded Gen3.5+ GFX Core, 400-MHz render clock frequency, up to 224 MB shared memory. Hard-drive: 32GB SSD drive. Its operating system is Ubuntu 12.04 LTS. Communication with an external computer is done via Ethernet and/or Wi-fi. Communication with actuators and sensors is via EtherCAT, The vehicle has four mecanum wheels

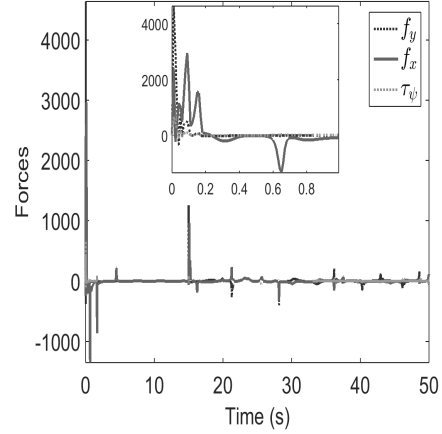


Figure 4. Generalized forces.

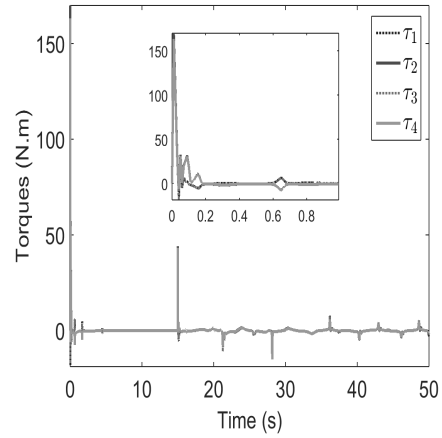


Figure 5. Motor torques.



Figure 6. Kuka-Youbot platform.

with radius of 47.5 mm , overall length: 580 mm , overall width: 380 mm . Height: 140 mm , Maximum velocity: 0.8 m/s . Weight: 20 Kg Power supply: 24 v DC . Payload: 20 Kg , Motor controller boards: Trinamic TMC series. The encoders accomplish 400 Counts per Revolution in all motors, from which position and velocity can be read.

Since the platform is able to receive torque signals, a torque-mode controller is implemented for the Kuka-Youbot vehicle alone, using a nominal PD controller similar to (44), with proportional gain $K_P = 200$ and derivative gain $K_D = 150$. Even though the manipulator arm was mounted on the platform, only the vehicle was

controlled, such that we can verify that the torque inputs in the generalized space are properly mapped to the space of the wheels. The given task has three stages; The first stage begins at $t < 0$, where the vehicle's initial coordinates are $\mathbf{x}(t) = [x \ y \ \psi] = [0 \ 0 \ 0]$, which must follow a trajectory defined by $\mathbf{x}_{l_d} = [2 \sin(t/2) \ \sin(t) \ 0]$, $\dot{\mathbf{x}}_{l_d} = [\cos(t/2) \ \cos(t) \ 0]$, $\ddot{\mathbf{x}}_{l_d} = \left[\frac{-\sin(t/2)}{2} \ -\sin(t) \ 0 \right]$. Then the second stage begins at $t \geq 25 \text{ s}$, where the task becomes a regulation task, $\mathbf{x}_{r_d} = [0 \ 0 \ 0]$, i.e., the vehicle moves towards the origin. Finally, the third stage begins as the vehicle is at the origin, where it must follow another trajectory defined by $\mathbf{x}_{c_d} = [\cos(t) \ \sin(t) \ 0]$, $\dot{\mathbf{x}}_{c_d} = [-\sin(t) \ \cos(t) \ 0]$, $\ddot{\mathbf{x}}_{c_d} = [-\cos(t) \ -\sin(t) \ 0]$. Figure (7a) shows the reference path generated by the three stages of the task, and the path generated by the robot when following the reference path, displaying a decently small error in the tracked coordinates x and y , and a very small error in the regulated coordinate ψ as seen in Figure (7b). Figures (8a) and (8b), show respectively the torque control inputs for each wheel required to achieve the task, which are computed from the control input of generalized forces through the mapping operator \mathbf{J}_b^+ .

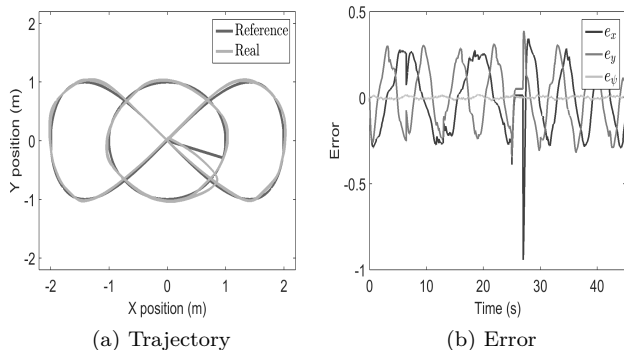


Figure 7. Kuka Youbot Vehicle's trajectory.

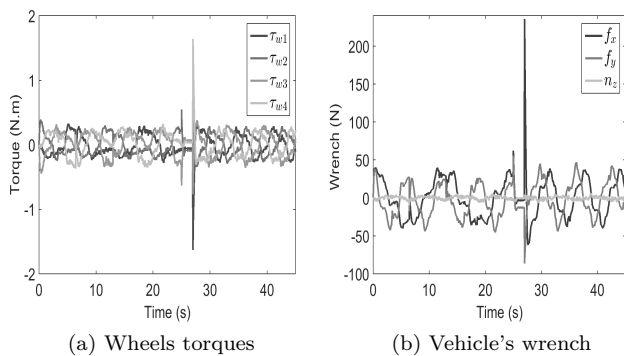


Figure 8. Kuka Youbot Vehicle's forces.

7. CONCLUSIONS

In this work we have demonstrated the usefulness of the force mapping operator obtained from the dynamic

model of the omnidirectional vehicle. This was proven successfully through simulations and real experiments. Both required the generalized control signals to be mapped into torque signals for the wheels, which move the vehicle as expected to fulfill the given tasks. This methodology leads to a formulation that can be easily modified for omnidirectional vehicles with a different amount and/or arrangement of wheels, by just characterizing the wrench of each individual wheel, transforming it from their local frame to the vehicle's frame, and finally adding them. This would lead to a new suitable force mapping operator.

Proper gain values must be obtained through a conventional tuning methodology, since the gains were tuned empirically in both simulations and experiments. However, along the task execution, the vehicle is proven to be stable through experiments with tracking tasks that require considerable changes of motion.

REFERENCES

- F.C. Park, J.E. Bobrow. and S.R. Ploen. A Lie Group Formulation of Robot Dynamics. *The International Journal of Robotics Research*, Volume 14, pages 609–618, 1995.
- R. Featherstone, and D. Orin. Robot Dynamics: Equations and Algorithms. *IEEE Int. Conf. Robotics and Automation*, pages 826–834, 2010.
- V. Estopier, G. Arechavaleta, and E. Olguín. Generación de Movimientos Humanoides con Dinámica Inversa Jerárquica *Congreso Latinoamericano de Control Automático 2014*.
- F. Mirelez-Delgado, A. Morales-Díaz, and R. Ríos-Cabrera. Kinematic control for an omnidirectional mobile manipulator. *Memorias del Congreso Nacional de Control Automático*, Septiembre 2016, Querétaro, México, 343–348.
- Sharma, S., Kraetzschmar, G.K., Scheurer, C., and Bischoff, R. Unified Closed Form Inverse Kinematics for the KUKA youBot. *Robotics; Proceedings of ROBOTIK 2012; 7th German Conference on*, 1–6.
- Changwu Qiu, and Qixin Cao. Modeling and Analysis of the Dynamics of an Omni-directional Mobile Manipulators System *J Intell Robot Syst (2008)* 52:101–120.
- K. Watanabe, K. Sato, K. Izumi, and Y. Kunitake. Analysis and Control for an Omnidirectional Mobile Manipulator *Journal of Intelligent and Robotic Systems* 27: 3–20, 2000.